Alexandria Engineering Journal (2016) 55, 2035–2043

HOSTED BY

ELSEVIER

Alexandria University

Alexandria Engineering Journal

www.elsevier.com/locate/aej
www.sciencedirect.com

ORIGINAL ARTICLE

Aerodynamic shape optimization and analysis of small wind turbine blades employing the Viterna approach for post-stall region

Arash Hassanzadeh [a,*], **Armin Hassanzadeh Hassanabad** [b], **Abdolrahman Dadvand** [c]

[a] *School of Mechanical Engineering, Iran University of Science and Technology (IUST), Tehran, Iran*
[b] *Department of Electrical Engineering, Kamal Institute of Technology, Urmia, Iran*
[c] *Department of Mechanical Engineering, Urmia University of Technology (UUT), Urmia, Iran*

Received 9 February 2016; revised 1 June 2016; accepted 11 July 2016
Available online 27 July 2016

KEYWORDS

Wind turbine blade;
BEM theory;
Shape optimization;
Annual Energy Production;
Post-stall airfoil data

Abstract This paper aims to optimize the distribution of chord and twist angle of small wind turbine blade in order to maximize its Annual Energy Production (AEP). A horizontal-axis wind turbine (HAWT) blade is optimized using a calculation code based on the Blade Element Momentum (BEM) theory. A difficult task in the implementation of the BEM theory is the correct representation of the lift and drag coefficients at post-stall regime. In this research, the method based on the Viterna equations was used for extrapolating airfoil data into the post-stall regime and the results were compared with various mathematical models. Results showed the high capability of this method to predict the performance of wind turbines. Evaluation of the efficiency of wind turbine blade designed with the proposed model shows that the optimum design parameters gave rise to an increase of 8.51% in the AEP rate as compared with the corresponding manufactured operating parameters.

1. Introduction

Due to increasing environmental concern and oil price and concerns over limited fossil-fuel resources, more and more electricity is being generated from renewable sources. Wind energy has been proved to be an important source of clean and renewable energy for producing electrical energy and special interest is paid toward wind energy due to its advantages [1]. The sustainability, reliability, and risk management of wind energy applications were studied by BoroumandJazi et al. [2]. Even for moderate wind speeds, the use of wind turbines is a very attractive way of generating electricity [3].

It has been shown that the major aspects of wind turbine performance (power output and loads) are determined by the aerodynamic forces generated by the wind. So, the turbine design is the most important step in developing the wind energy industry. Numerous computational approaches have been applied to aerodynamic design of wind turbines such as blade element momentum (BEM) theory, vortex wake method, and computational fluid dynamic (CFD). Among these computational approaches, the BEM theory is widely used to

* Corresponding author.
E-mail address: ahasanzadeh.iust@gmail.com (A. Hassanzadeh).
Peer review under responsibility of Faculty of Engineering, Alexandria University.

http://dx.doi.org/10.1016/j.aej.2016.07.008

Nomenclature

A	swept area of rotor	R	wind rotor radius
a	axial induction factor	Re	Reynolds number
a'	tangential induction factor	T	thrust
c	airfoil chord	U	wind speed
C_D	drag coefficient	α	angle of attack
C_L	lift coefficient	θ_T	section twist angle
C_p	power coefficient	φ	angle of relative wind
c'	Weibull scale parameter	σ	local solidity
F	tip loss factor	ρ	air density
k	Weibull shape parameter	λ	tip speed ratio
M	torque	ω	angular velocity
N_b	number of blades	AEP	Annual Energy Production
P	power	AR	Aspect Ratio
$p(U)$	wind speed probability density function	DUT	Delft University of Technology
r	blade local radius		

aerodynamic design of wind turbines due to its simplicity and accuracy [4]. The BEM theory is based on the Glauert propeller theory [5], which has been modified for application to wind turbines.

Optimization methods based on BEM theory provide good solutions with less computational cost [6]. Several works have been carried out on wind turbine blade shape optimization [7–11]. A comprehensive review of wind turbine optimization techniques is given by Chehouri et al. [12]. The aerodynamic performance optimization of horizontal axis wind turbine blades using BEM theory and genetic algorithm (GA) has been performed by Ceyhan [7]. The chord and twist angle distribution are considered as design variables and optimized for optimum power production. Kenway and Martins [8] applied a multidisciplinary design feasible (MDF) approach to optimize wind turbine blade shape. A possible output increase of 3–4% was obtained for a 5 kW wind turbine, demonstrating the potential of the optimization method. Clifton-Smith and Wood [9] employed a differential evolution method to improve both the power and the starting performance. The goal was to maximize the power coefficient and to minimize the starting time for small wind turbine blades. Liu et al. [10] developed an optimization method for wind turbine blades to maximize annual power production. In their work, the geometric blade shape design and blade performance optimization were done and an increase of 7.5% in the annual energy output was recorded.

Wind turbine blade shape optimizations are mostly conducted for wind turbines working in on-design conditions. However, wind turbines are exposed to various wind conditions, thus sometimes working at post-stall region. A difficult goal in the implementation of the BEM theory in the post-stall region is the correct representation of the lift and drag coefficients. Therefore, providing reliable airfoil data, especially post-stall values of aerodynamics coefficients that characterize the blade loading seems necessary.

In the present work, a mathematical model based on the Viterna method [13] is implemented for post-stall region and the performance of the simulated model in terms of lift and drag coefficients is compared with different available mathematical models. The implementation of this model offers the possibility to design the wind turbine and analyze its performance in on-design and off-design conditions at a wide range of wind velocities and different wind conditions. This is specifically good for stall-regulated wind turbines which use reduction in lift force to control the amount of power extracted from wind. The implemented method is then utilized to optimize the distributions of chord and twist angle of horizontal-axis wind turbine (HAWT) blade. An optimization model for blades of HAWTs is presented that accounts for the wind speed distribution function of the specific wind site in Iran targeting the maximum Annual Energy Production (AEP).

2. Numerical method

The methodology used in the present work is a combination of a computational code (i.e., BEM theory) and an optimization model (i.e., GA). The former is used for aerodynamic analysis of the wind turbine blade and the latter is utilized for optimization of the wind turbine blade shape.

2.1. Computational code

In this work, the BEM theory is used for the aerodynamic design of a wind turbine. The BEM theory comprises two parts. In the first part, the model divides the blade into several independent elements (sections) along the length as shown in Fig. 1. It further assumes that the aerodynamic forces on each element can be calculated as a two-dimensional airfoil subjected to the flow conditions. A cross section of a rotor blade located at radius r of the blade element is shown in Fig. 2, which is provided with associated velocity and force components. Thrust and torque can be obtained from the aerodynamic forces on the cross section of the rotor blade as a function of tangential and axial induction factors a and a':

$$dT = \frac{\rho}{2}\frac{U^2(1-a)^2}{\sin^2\varphi}N_b(C_L\cos\varphi + C_D\sin\varphi)c\,dr \tag{1}$$

$$dM = \frac{\rho}{2}\frac{U(1-a)}{\sin\varphi}.\frac{\omega r(1+a')}{\cos\varphi}N_b(C_L\sin\varphi - C_D\cos\varphi)cr\,dr \tag{2}$$

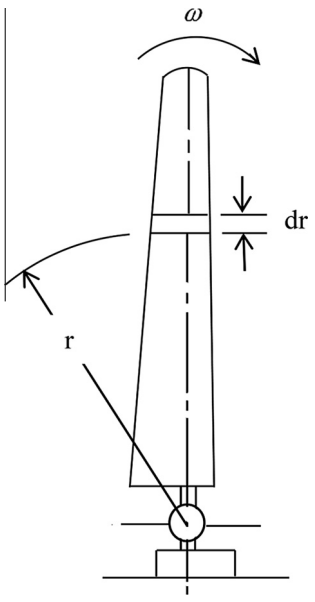

Figure 1 Schematic of blade elements.

In the second part, by applying the conservation of momentum, the net force on the actuator disk is obtained from the change of air momentum passing through the disk, and the rate of momentum is equivalent to the air velocity difference across the rotor plane times the mass flow rate. Hence, the thrust and torque of the blade can be obtained as follows:

$$dT = 4\pi r\rho U^2 a(1-a)dr \tag{3}$$

$$dM = 4\pi r^3 \rho U\omega(1-a)a'dr \tag{4}$$

By setting Eqs. (1) and (2) respectively equal to Eqs. (3) and (4), the axial and tangential induction factors can be found as follows:

$$a = \frac{1}{\frac{4F\sin^2\varphi}{\sigma(C_L\cos\varphi + C_D\sin\varphi)} + 1} \tag{5}$$

$$a' = \frac{1}{\frac{4\sin\varphi\cos\varphi}{\sigma(C_L\sin\varphi - C_D\cos\varphi)} + 1}, \tag{6}$$

where F is the Prandtl tip loss correction factor. An approximate formula for the Prandtl tip loss function was introduced by Glauert [14] as,

$$F = \frac{2}{\pi} ar\cos\left[\exp\left(\frac{N_b(r-R)}{2r\sin\varphi}\right)\right] \tag{7}$$

where σ is the local solidity defined as follows:

$$\sigma = \frac{cN_b}{2\pi r} \tag{8}$$

Eq. (5) gives reliable results only for axial induction factor values between 0 and 0.4. For axial induction factors greater than 0.4 the BEM theory does not yield reliable results. To correct the axial induction factor when $a > 0.4$, Eq. (9) is used as proposed in Ref. [15]:

$$a = \frac{18F - 20 - 3\sqrt{C_N(50-36F) + 12F(3F-4)}}{36F - 50} \quad \text{for } a > 0.4 \tag{9}$$

Airfoil behavior is normally classified into three flow regimes: the attached flow regime, the high lift/stall development regime, and the flat plate/fully stalled regime [16]. The dimensionless coefficients for the S809 airfoil resulting from tests taken at Delft University of Technology (DUT) [17] are used for BEM analysis at angles of attack below stall (the attached flow regime). For this purpose, a complete table of airfoil coefficients, spanning from −180° to 180° is needed. In order to estimate airfoil behavior at high positive and negative angles of attack other methods must be employed. A method based on the Viterna equations is used for extrapolating airfoil data into the high lift/stall development regime.

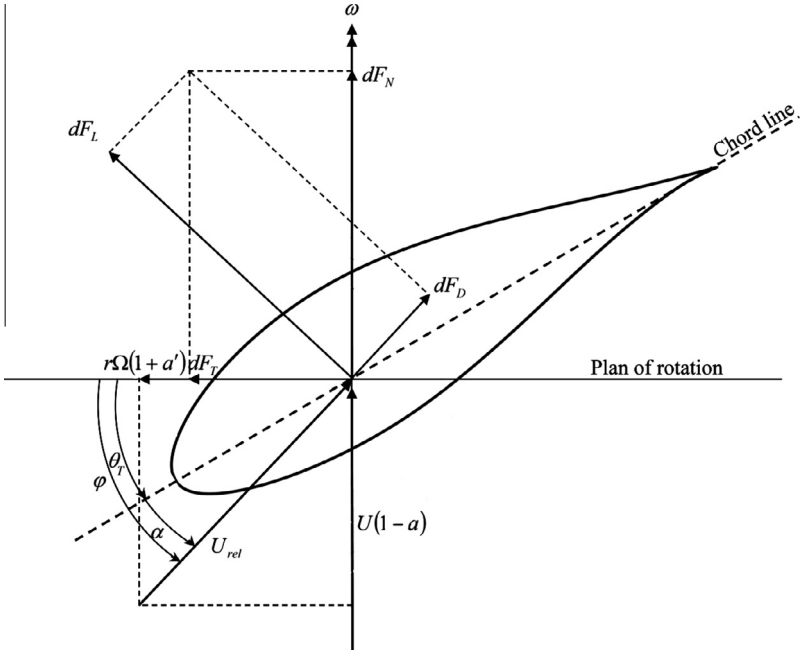

Figure 2 Blade element geometry and the velocity and force components.

For $\alpha_{stall} \leqslant \alpha \leqslant 90^{\circ}$, the drag and lift coefficients are calculated as follows [18],

$$C_D = B_1 \sin^2 \alpha + B_2 \cos \alpha$$
$$C_L = A_1 \sin 2\alpha + A_2 \frac{\cos^2 \alpha}{\sin \alpha} \quad (10)$$

where

$$B_1 = C_{D\max} = 1.11 + 0.018AR \quad (\alpha = 90^{\circ})$$

$$B_2 = \frac{C_{D\,stall} - C_{D\max} \sin^2 \alpha_{stall}}{\cos \alpha_{stall}}$$

$$A_1 = B_1/2$$

$$A_2 = (C_{L\,stall} - C_{D\max} \sin \alpha_{stall} \cos \alpha_{stall}) \frac{\sin \alpha_{stall}}{\cos^2 \alpha_{stall}}$$

Fig. 3 shows the lift and drag coefficients associated with the S809 airfoil for aspect ratio of 14 (AR = 14) at the range of angle of attacks considered in the present work. This is a combination of the data obtained from experiment (DUT data [17]) and predicted by Viterna equation. It may be noted that, the experimental results are used for BEM analysis at angles of attack below stall. The result represents that at the angle of attack of 45°, the Cl is equal to Cd, which is consistent with flat plate theory.

For angles of attack between 90° and 180° (positive or negative), the lift and drag coefficients are approximated as the flat plate/fully stalled regime values [19]:

$$C_{L\,plat} = 2 \sin \alpha \cos \alpha \quad (11)$$

$$C_{D\,plat} = 2 \sin^2 \alpha \quad (12)$$

The algorithm of BEM theory for each element of the blade can be summarized as the following 7 steps:

Step 1: Initialize a and a',
Step 2: Compute the inflow angle,
Step 3: Calculate the local angle of attack by subtracting twist angle from inflow angle,
Step 4: Read aerodynamic coefficients from tabulated airfoil data,
Step 5: Compute a and a' from Eqs. (5) or (9) and (6),
Step 6: If a and a' have changed more than a certain tolerance, go to Step 2, otherwise continue,
Step 7: Compute aerodynamic loads.

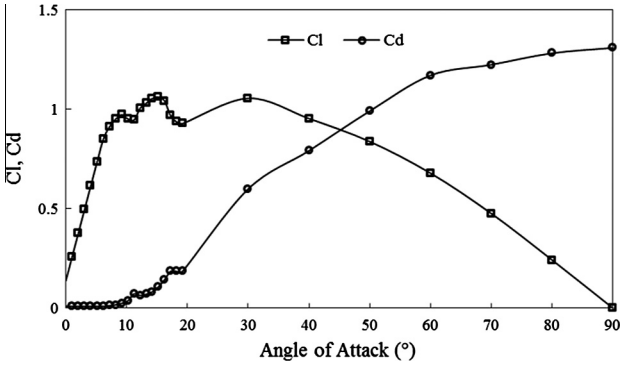

Figure 3 Lift and drag coefficients vs. angle of attack associated with the S809 airfoil for AR = 14.

2.2. Optimization model

2.2.1. Genetic algorithm

The genetic algorithm is a non-gradient based algorithm for solving both constrained and unconstrained optimization problems that are based on natural selection. It is inspired by Darwin's theory about evolution. The genetic algorithm repeatedly modifies a population of individual solutions. At each step, the genetic algorithm selects individuals at random from the current population to be parents and uses them to produce the children for the next generation. Over successive generations, the population "evolves" toward an optimal solution. Population is governed by natural selection with crossover, reproduction and mutation operations. Genetic algorithm is a popular optimization method for many engineering problems, in which wind turbine shape optimization is one of them. In the general case, the optimization is defined as follows:

$$x = (x_i) \quad \forall i = 1, 2, \ldots N.$$

Minimize $f(x)$

$$h_j(x) \leqslant 0 \quad \forall j = 1, 2, \ldots n.$$

Here, x, N, $f(x)$ and $h_j(x)$ are design parameters vectors, number of design parameters, objective function and unequal constraints respectively.

2.2.2. Objective function

The annual energy output equals the product of the average power of the wind turbine and the constant time of one year. Thus, annual average power can be used as the design objective, and the fitness function AEP can be defined as [20]:

$$\mathrm{AEP} = 8760 \int_0^{\infty} Power(U)\, p(U)\, dU \quad (13)$$

where $Power(U)$ and $p(U)$ are the mechanical power of the wind turbine and the probability of wind speed occurrence, respectively and are defined as follows. A mechanical torque is produced when air passes through the turbine blades. This torque is used to produce power. The mechanical power of the wind turbine extracted from the wind is expressed as,

$$Power(U) = \frac{1}{2} C_{power} \rho A U^3 \quad (14)$$

where ρ is air density, A is the swept area of rotor, U is wind speed and C_{power} is the power coefficient. The power coefficient is a function of tip speed ratio λ defined as the ratio between the blade tip speed and the wind speed:

$$\lambda = \frac{R\omega}{U} \quad (15)$$

The probability of wind speed occurrence is determined by the Weibull probability distribution curve [16]:

$$p(U) = \left(\frac{k}{c'}\right)\left(\frac{U}{c'}\right)^{k-1} \exp\left[-\left(\frac{U}{c'}\right)^{k}\right], \quad (16)$$

where c' denotes Weibull scale parameter and k is Weibull shape parameter.

2.2.3. Decision variables

The shape of a blade is determined by the airfoil, chord length and twist angle of each blade section. When the airfoil family is defined, it needs to get the optimal chord length and twist angle distributions along the blade. To achieve smooth spanwise distributions of chord length and twist angle in the main power production part of the blade, both distributions are defined as a function of blade radius using the Bezier curve. The Bezier curves defining the distributions of chord length and twist each uses five control points. Thus, there are ten decision variables in total.

2.2.4. Constraints

The upper and lower bounds of chord length and twist angle as geometrical design parameters are presented respectively in Figs. 4 and 5. The specific limits for design parameters ensure that acceptable blade geometries are produced.

2.3. The combination of BEM and genetic algorithm

The combination of flow analysis by BEM code and optimization procedure by Genetic algorithm (GA) is shown in Fig. 6. The optimization program provides the BEM code with the new value of the design variables (new geometrical data for blade); then, the value of objective function (AEP) is obtained from BEM code. The optimization program modifies the design variables and runs the BEM program again. This procedure continued until satisfying the optimization convergence conditions and reaching to desired geometry for the blade.

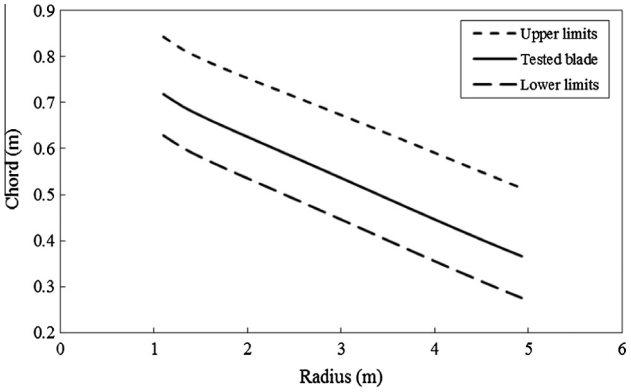

Figure 4 Upper and lower chord length limits.

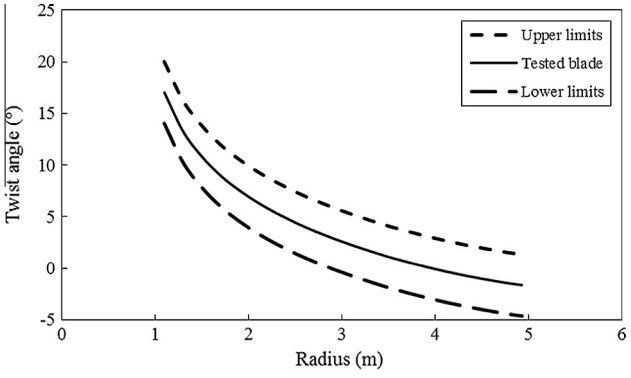

Figure 5 Upper and lower twist angle limits.

3. Results and discussion

In this section, first the accuracy of the mathematical code is substantiated through the comparison of the predicted results with the available experimental data. Then the current numerical results are compared with those obtained from different mathematical models proposed by others. Finally, the turbine blade is optimized using the genetic algorithm (GA) to produce maximum AEP.

3.1. Model verification

The accuracy of the results obtained from the current mathematical code is substantiated through the comparison with the experimental data from the UAE research wind turbine reported in [21]. In the experiments, a two-bladed UAE Phase VI wind turbine with a 10 m diameter rotor was placed in the 24×36 m wind tunnel for pressure measurements along the blade. The rotor was turned clockwise at a constant speed of 71.6 rpm, it was stall regulated and blade pitch was held constant at 3°. The results are depicted in Figs. 7 and 8, demonstrating the high capability of the implemented approach in predicting the power coefficient and power of wind turbine.

The differences between the predicted and measured power are depicted in Fig. 9 for different wind speeds. Fig. 9 shows the overall discrepancy between the simulated results and the experimental data are less than 10%. In addition, the minimum discrepancy is found to be 0.02% happening at $V = 13.1$ m/s.

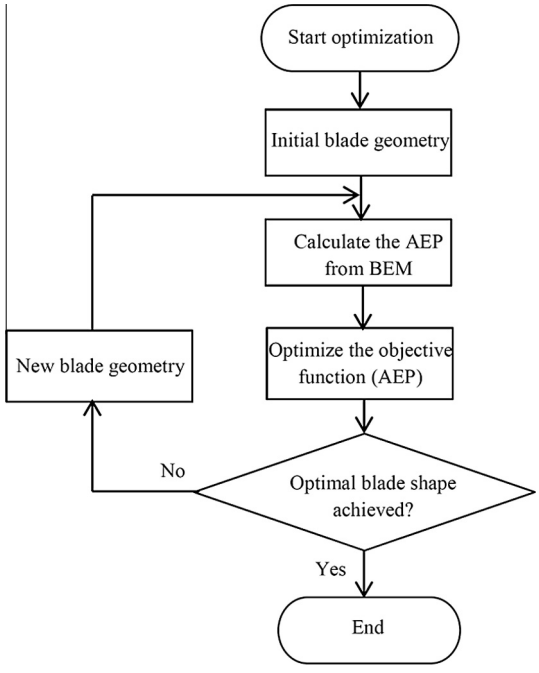

Figure 6 Flowchart of optimization procedure.

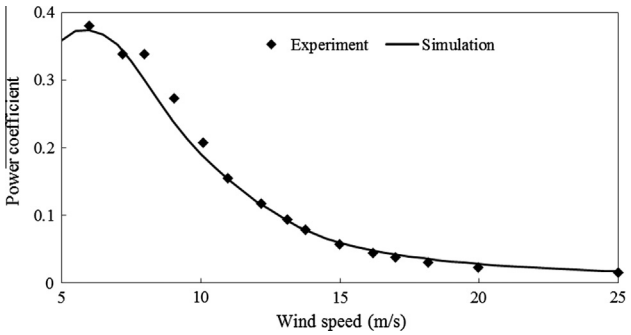

Figure 7 Comparison between results of experimental power coefficient for the NREL wind turbine [21] and the present simulated data.

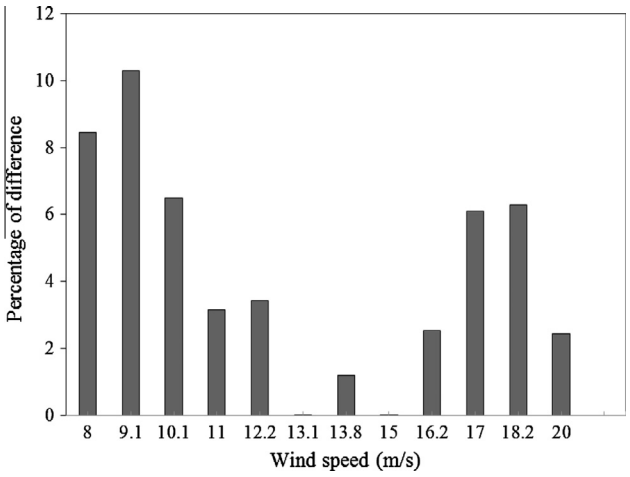

Figure 9 Percentage of difference between the experimental and simulated power.

3.2. Comparison of the current results with those from different mathematical models

The BEM theory uses the lift and drag coefficients associated with the airfoils of turbine blade to evaluate the performance of the rotor. The airfoil data resulting from the experimental tests are used for BEM analysis only at the attached flow regime. However, the method described by Tangler and Kocurek [13], which was also used in the present work can be utilized to find the aerodynamic coefficients in the stall regions. Furthermore, in the recent years, various mathematical models were proposed to describe the correct trend of lift and drag coefficients at the stall regions. These models are articulated as follows:

- BEM with C_L 2D: BEM Theory with C_L and C_D measured in the wind tunnel;
- Wilson et al. [22];
- Viterna and Corrigan [23];
- CL 3D + hub losses [24];
- EOLO [4].

In Fig. 10 a comparison has been made between the current simulated results and those obtained from different mathematical models and the experimental data of [21]. The results show that the simulated approach in this work exhibits higher capability in predicting the performance of wind turbines and attempts to explain the 3-D aerodynamics that exists before and after peak rotor power.

3.3. Optimization results

The performance of the GA is summarized in Fig. 11 in terms of the increase in fitness of the population. This figure is associated with the best fitness of AEP vs. generation. It can be seen that the maximum fitness increases in steps interspaced by long periods of stagnancy. This trend implies that the GA is going to improve the population on a consistent basis.

As for our case study, we considered the Ahar city located in the province of East Azerbaijan in Iran. The values of k and c are calculated to be 1.57 and 7.34, respectively [25]. Weibull probability density function for all of the velocities within the operating range of the turbine is shown in Fig. 12. Fig. 13 shows the chord and twist distributions of the tested and optimized virtual UAE wind turbine rotor. It can be seen from Fig. 13A that, the values of chord for optimized rotor are greater than their original rotor counterparts. In addition, the discrepancy between the tested and optimized rotor chord increases by moving toward the tip of the blade. Fig. 13B reveals that the twist angle is almost the same for both the

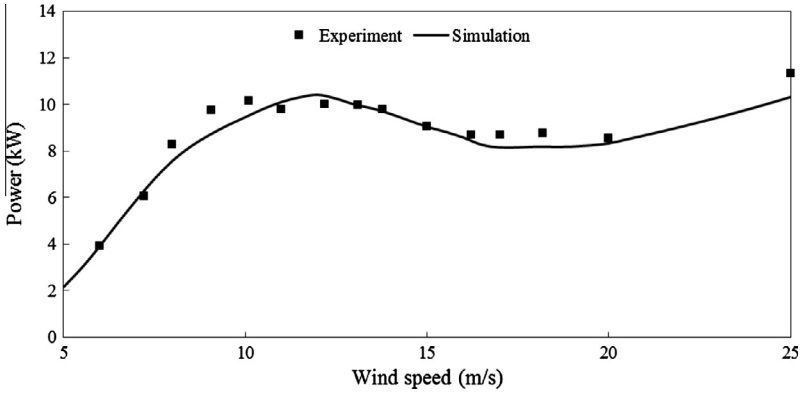

Figure 8 Comparison between results of experimental mechanical power for the NREL wind turbine [21] and present simulated data.

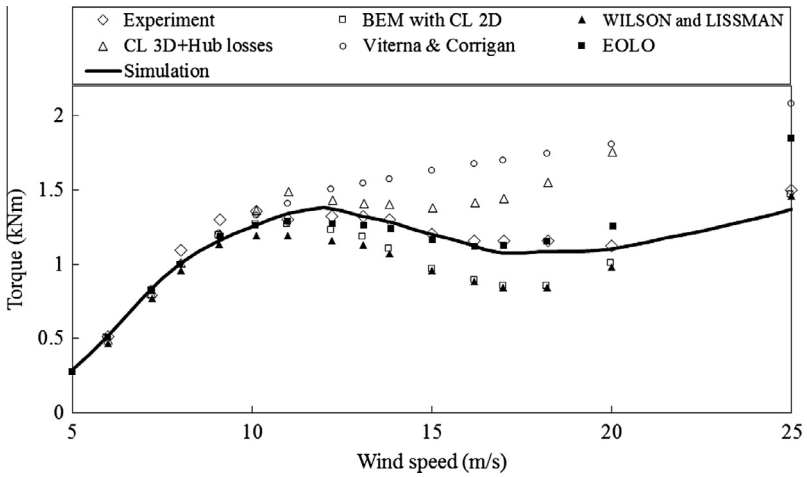

Figure 10 Comparison of the current simulated results with the experimental data of [21] and the results of different mathematical models.

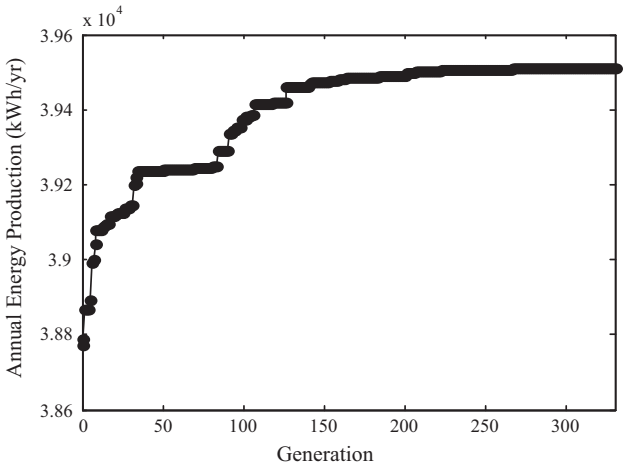

Figure 11 Convergence of the annual energy production for GA-based optimization algorithm.

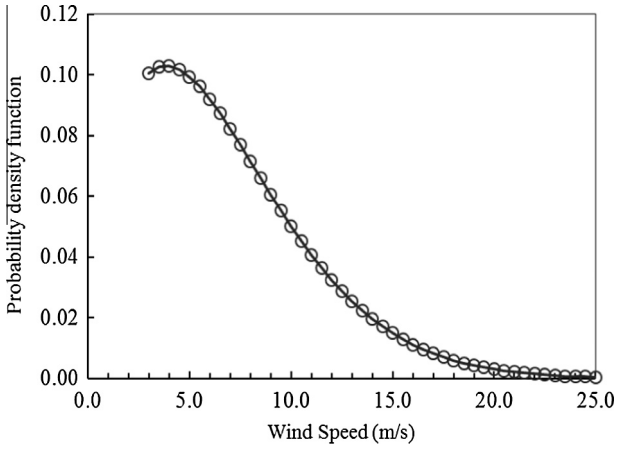

Figure 12 Probability density function versus wind speed for our case study.

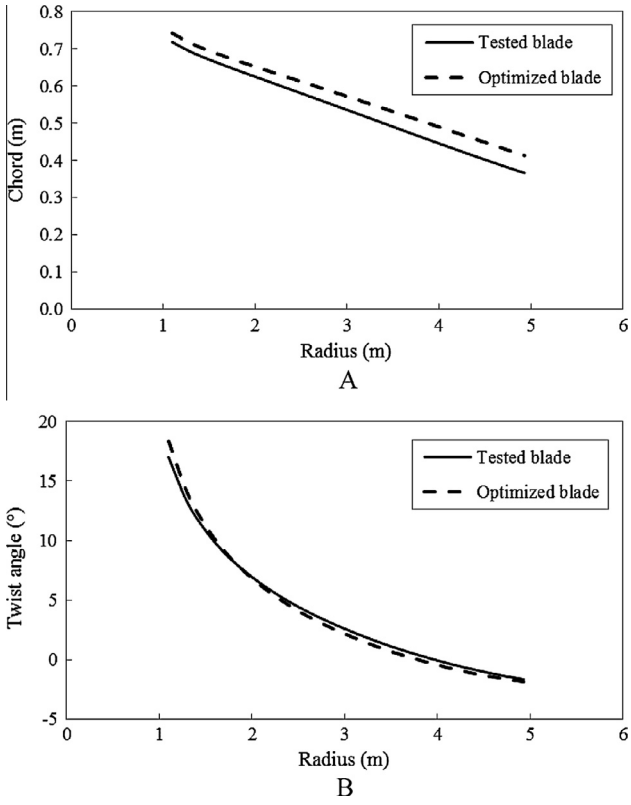

Figure 13 Chord variations (A) and twist angle variations (B) along the blade length for the tested and optimized blades.

tested and optimized blades and only trivial difference is observed.

The comparison between the power coefficient associated with the tested and optimized blade has been shown in Fig. 14. It can be seen that the power coefficient increases as the wind speed increases from 4 to 12 m/s. This is very important from practical point of view due to the fact that the probability density function is high in this range of wind velocity. The power coefficient reaches its maximum value at around

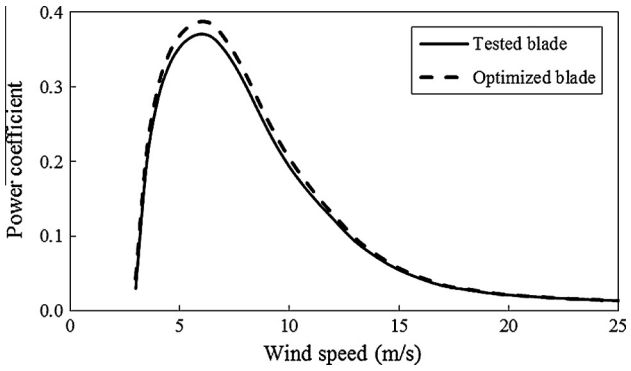

Figure 14 Comparison between the power coefficients associated with the tested and optimized blade.

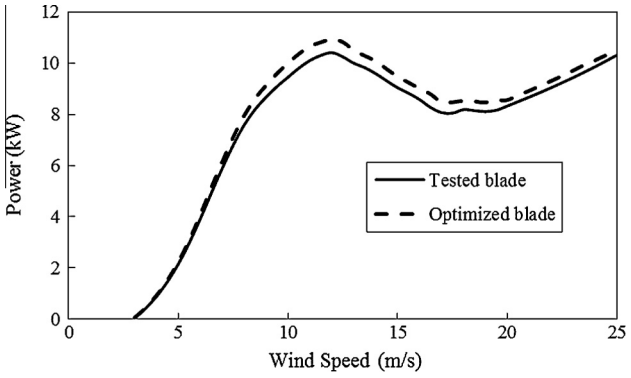

Figure 15 Comparison between the powers associated with the tested and optimized blade.

6 m/s. This maximum value is 0.371 for the tested rotor and 0.388 for the optimized rotor.

As it can be observed from Figs. 14 and 15, the optimized blade has higher power coefficient and power curve compared to the tested one. Thus, it is expected to have a high AEP for the optimized wind turbine. The AEP is related to the mechanical power of the wind turbine and the probability of wind speed occurrence. By optimizing the blade shape, the mechanical power of wind turbine is increased (see Fig. 15). In order to obtain real value for AEP, the probability density function of wind speed in Ahar city located in the province of East Azerbaijan in Iran is considered. 200 discrete points are specified between cut-in velocity of 5 m/s and cut-out velocity 25 m/s with a velocity step of 0.1. Based on the discrete form of AEP equation, $AEP = 8760 * \sum_{i=1}^{200} Power(u_i)p(u_i)\Delta u$, for known Power ($u_i$) and $p(u_i)$, the AEP values for the tested and the optimized rotors are calculated to be 36,413 and 39,510 kW h/year, respectively. In other words, the AEP has increased about 8.51% via optimization of the rotor blade.

4. Conclusions

In the present work, the blade of the UAE phase VI wind turbine was optimized. The BEM theory was used for flow analysis and the method described by Tangler and Kocurek [13] was used for predicting the aerodynamic coefficients of airfoils in the post-stall regime. The numerical results were compared with the available experimental data showing the capability of the current numerical method in predicting the flow physics. In addition, the current numerical method demonstrated superiority over the other mathematical methods. Then the UAE phase VI wind turbine blade was optimized. The optimized blade offers optimum aerodynamic design, and presents a higher power output gain between cut-in and cut-out velocities. The AEP values for the wind speed distribution in Ahar City were obtained to be 36,413 and 39,510 kW h/year, which are associated with the tested and the optimized rotors, respectively. In other words, the AEP has increased about 8.51% via optimization of the rotor blade.

References

[1] N.H. Mahmoud, A.A. EL-Haroun, E. Wahba, M.H. Nasef, An experimental study on improvement of Savonius rotor performance, Alexandria Eng. J. 51 (2012) 19–25.
[2] G. BoroumandJazi, B. Rismanchi, R. Saidur, Technical characteristic analysis of wind energy conversion systems for sustainable development, Energy Convers. Manage. 62 (2013) 87–94.
[3] D. Karamanis, Management of moderate wind energy coastal resources, Energy Convers. Manage. 52 (2011) 2623–2628.
[4] R. Lanzafame, M. Messina, Fluid dynamics wind turbine design: critical analysis, optimization and application of BEM theory, Renewable Energy 32 (14) (2007) 2291–2305.
[5] H. Glauert, The Elements of Airfoil and Airscrew Theory, Cambridge University Press, Cambridge, 1926.
[6] M.O.L. Hansen, Aerodynamics of Wind Turbines, second ed., Earthscan, London, UK, 2008.
[7] O. Ceyhan, Aerodynamic Design and Optimization of Horizontal Axis wind Turbines by using BEM Theory and Genetic Algorithm [Master Thesis], Aerospace Engineering Department, METU, Ankara, 2008.
[8] G. Kenway, J. Martins, Aerostructural shape optimization of wind turbine blades considering site-specific winds, in: Proc of 12th AIAA/ISSMO Multidisciplinary Analysis and Optimization Conference, University of Toronto Institute for Aerospace Studies, Victoria, 2008.
[9] M. Clifton-Smith, D. Wood, Further dual purpose evolutionary optimization of small wind turbine blades, J. Phys.: Conf. Ser., IOP Publishing, 2007, p. 012017.
[10] X. Liu, Y. Chen, Z. Ye, Optimization model for rotor blades of horizontal axis wind turbines, Front. Mech. Eng. China 2 (2007) 483–488.
[11] P. Fuglsang, H. Madsen, Optimization method for wind turbine rotors, J. Wind Eng. Ind. Aerodyn. 80 (12) (1999) 191–206, http://dx.doi.org/10.1016/S0167-6105(98)00191-3.
[12] A. Chehouri, R. Younes, A. Ilinca, J. Perron, Review of performance optimization techniques applied to wind turbines, Appl. Energy 142 (2015) 361–388.
[13] J.L. Tangler, J.D. Kocurek, Wind Turbine Post-Stall Airfoil Performance Characteristics Guidelines for Blade-Element Momentum Methods, in: 43rd AIAA Aerospace Sciences Meeting and Exhibit, Reno, NV, no. NREL/CP-500-36900, 2005.
[14] H. Glauert, Airplane propellers, in: W.F. Durand (Ed.), Aerodynamic Theory, Dover, New York, 1963, pp. 169–360.
[15] L. Buhl, Jr., A new empirical relationship between thrust coefficient and induction factor for the turbulent windmill state. Technical Report NREL/TP-500-36834, August 2005.
[16] J.F. Manwell, J.G. McGowan, A.L. Rogers, Wind Energy Explained Theory, Design and Application, John Willy & Sons, 2002.

[17] D.M. Somers, Design and Experimental Results for the S809 Airfoil. NREL/SR-440-6918, 1997.
[18] L.A. Viterna, D.C. Janetzke, Theoretical and Experimental Power from Large Horizontal-Axis Wind Turbines, TM-82944, September 1982.
[19] Richard W. Vesel Jr., Aero-Structural Optimization of a 5 MW Wind Turbine Rotor Master Thesis, The Ohio State University, 2012.
[20] E. Hau, Wind Turbines: Fundamentals, Technologies, Application, Economics, Springer Verlag, 2006.
[21] C. Lindenburg, Investigation into rotor blade aerodynamics. ECN-C-03-025, July 2003.
[22] R.E. Wilson, P.B. Lissaman, S.N. Walker, Aerodynamic Performance of Wind Turbines. Oregon State University, Report No. PB-259089, 1976.
[23] L.A. Viterna, R.D. Corrigan, Fixed Pitch Rotor Performance of Large Horizontal Axis Wind Turbines, in: DOE Workshop on Large Horizontal Axis Wind Turbines, OH, 1981.
[24] G.P. Corten, Flow Separation on Wind Turbine Blades PhD Thesis, Utrecht University, 2001.
[25] P. Alamdari, O. Nematollahi, M. Mirhosseini, Assessment of wind energy in Iran: a review, Renew. Sustain. Energy Rev. 16 (2012) 836–860.